Contribution ID: **1361** Type: **Regular Poster**

Divertor Heat Flux Broadening by Grassy ELMs

Friday 14 May 2021 12:10 (20 minutes)

The BOUT++ simulations of C-Mod, DIII-D, and EAST H-mode discharges follow the Heuristic-Drift-based (HD) empirical divertor heat flux width scaling of the inverse dependence on the poloidal magnetic field [1,2]. The BOUT++ simulations for ITER and CFETR indicate that divertor heat flux width λ_q of the future large machines may no longer follow the $1/B_{pol,OMP}$ scaling, while the HD model gives a pessimistic limit of divertor heat flux width as shown in Fig.1. The simulation results show a transition from a drift dominant regime to a fluctuation dominant regime from current machines to future large machines such as ITER and CFETR [3]. A threshold formula of thermal transport is derived for a transition from drift dominant regime to fluctuation dominant regime

$\chi_\perp^c = C\frac{2T_{e,sep}^{3/2}}{BB_pR}\frac{m_p^{1/2}}{e^2}\frac{a}{R}$,

where C=26.5 is a fitting parameter to simulations for the transition. When $\chi_\perp \ll \chi_\perp^c$, the heat flux width λ_q is a constant, the drifts dominate cross-field transport and heat flux width is insensitive to the turbulent transport χ, which is consistent with the Goldston HD model. When $\chi_\perp \gg< \chi_\perp^c$, heat flux width λ_q increases with χ, corresponding to fluctuation dominating cross-field transport. The threshold formula indicates two reasons for the transition. (1) The magnetic drift-based radial transport decreases due to large CFETR and ITER machine sizes and strong magnetic field. (2) The SOL fluctuation-driven thermal diffusivity increases due to larger turbulent fluxes ejected from the pedestal into the SOL when operating in a small and grassy ELM regime. The formula further indicates that by fixing the safety factor q_{95}, the separatrix temperature $T_{e,sep}$, the inverse aspect ratio (a/R), and the machine size R, the critical value of thermal diffusivity $\chi_\perp^c$ is inversely proportional to the square of the poloidal magnetic field $B_p(\chi_\perp^c\ 1/B_p^2)$. Therefore, a reduction of poloidal magnetic field or plasma current by a factor of 3 from ITER baseline target scenario would lead to a 9 times higher critical value of thermal diffusivity $\chi_\perp^c$, possibly yielding a transition from fluctuation to drift dominant regime. BOUT++ transport simulations confirm the analytical estimate for the transition, as shown in Fig.1 as a large green star for $B_{pol,MP} = 0.42T$. More BOUT++ ITER turbulence simulations will be presented to confirm the transitions for the ITER scenarios in Pre-Fusion Power Operations, such as PFPO-1 and PFPO-2, and Steady State Operation. Even for present tokamaks, there is evidence that the divertor heat flux width can have a significant departure from the HD model and the empirical scaling predictions. Recent DIII-D grassy ELM experiments show a consistent divertor heat flux width broadening and amplitude reduction on the inner target [4], as predicted by BOUT++ simulations. From the ELM-free phase to the grassy ELM phase with RMP, the time-averaged divertor heat flux width increases up to 6 times, while the divertor heat flux width features strong fluctuations during the type-I intra-ELM phase. The natural grassy-ELMs with the no-RMP case show a similar broadening with 2-3 times divertor heat flux width in the ELM-free phase. The excitement about the grassy-ELM regime is that the global confinement is maintained and the peak heat flux at the divertor targets is reduced by a factor of 10 in comparison with type-I ELMs as demonstrated in EAST, JT-60U, and TCV experiments. Recent linear and nonlinear BOUT++ simulations on EAST experiments have revealed, for the first time, that the key mechanism for the grassy ELMs is the expansion of the peeling boundary into a stable region due to radially localized steepening in the pedestal pressure gradient triggered by a radially localized collapse [5], based on the well-known effect of kink/peeling mode stabilization by pressure gradient. For type-I ELMs, the high current density and gradient drive the kink/peeling-dominated low-n PBMs instability. During ELM crash cases, the collapsing front propagates radially inward, leading to large ELMs, as observed by the Lithium BES on EAST. For grassy ELMs, the pedestal current density and gradient are inherently lower, and the operational parameter space can intrinsically improve the pedestal stability against the low-n PBMs. Hence, the instabilities quickly dissipate as the pressure gradient is just slightly reduced, leading to small ELMs. The grassy ELM regime is particularly suited for a high magnetic field steady-state tokamak reactor, such as the CFETR with q_{95} = 5.5-7, β_p=2, $f_{GW} \simeq 0.7-1.2$, $\delta_{95} \simeq 0.4-0.5$, and $\nu_{*ped} \leq 0.3-0.8$ [6]. Even though the ITER baseline operation scenario is in the type-I ELMy H-mode regime for the highest fusion power with the highest current and the highest pedestal temperature, the parameters for ITER steady-state op-

eration scenario with lower current ($q_{95} = 5.3, \beta_p = 1.65, f_{GW} \simeq 0.82, \delta_{95} \simeq 0.5$) are in principle consistent with those for achieving the grassy ELMs. BOUT++ six-field two-fluid turbulence code is applied for simulations of different ITER scenarios, namely 15 MA baseline, 11.5MA hybrid and 10MA SSO (Steady-State Operation). The most unstable modes in linear stage show that different peeling-ballooning instabilities dominate in the three scenarios, with the baseline scenario has the most unstable toroidal mode numbers in the range of n=60 80 with characteristics of ballooning modes, the hybrid scenario has the most unstable modes at n 40, and for the SSO scenario the most unstable modes are in the range of n=15 20 with characteristics of peeling modes. The nonlinear simulations yield different types of ELMs in the final nonlinear phases. The energy loss fractions in the baseline and hybrid scenarios are large (10-20

[1.] Goldston R.J. 2012 Nucl. Fusion 52 013009; [2.] Eich T. et al Nucl. Fusion 53 (2013) 093031; [3] X.Q. Xu, et al Nucl. Fusion 59 (2019) 126039; [4] Nazikian, et al. Nucl. Fusion 58 (2018) 106010; [5] G S Xu, et al., Phys. Rev. Lett. 122, 255001 (2019); [6] E. Viezzer, Nucl. Fusion, vol. 58, 115002 (2018). [7] J.P. Gunn, et al Nucl. Fusion 57 (2017) 046025. [8] N. Oyama, Journal of Physics: Conference Series 123 (2008) 012002.

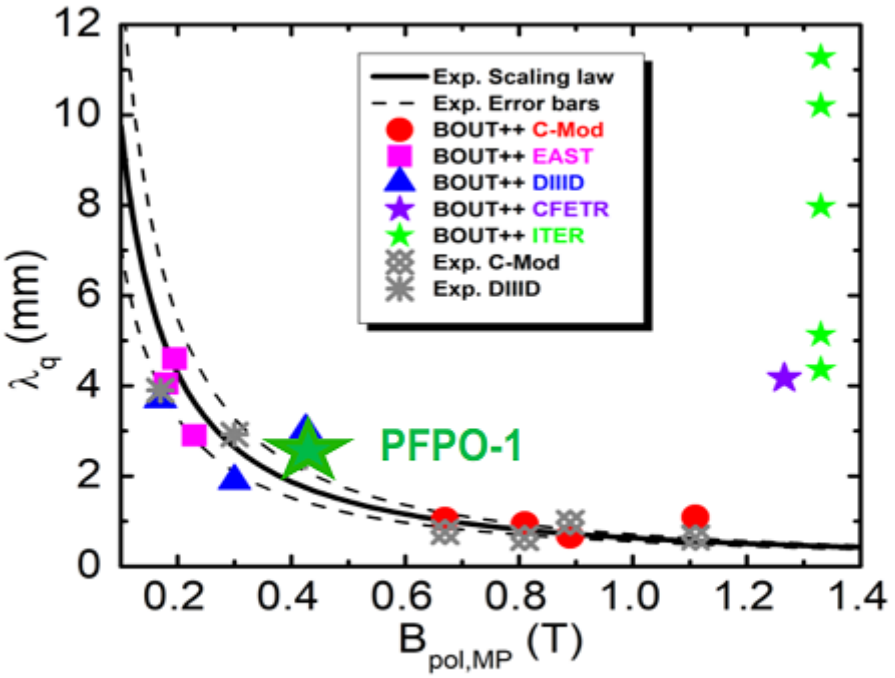

FIGURE 1: Divertor heat flux width λ_q vs. poloidal magnetic field at outer midplane $B_{pol,MP}$. The five green stars for ITER baseline scenario correspond to scan of pedestal heights, from original pedestal profiles to the reduced pedestal height at 95%, 90%, 85%, and 80%. The large green star for ITER PFPO-1 scenario is from BOUT++ transport simulations.

Figure 1:

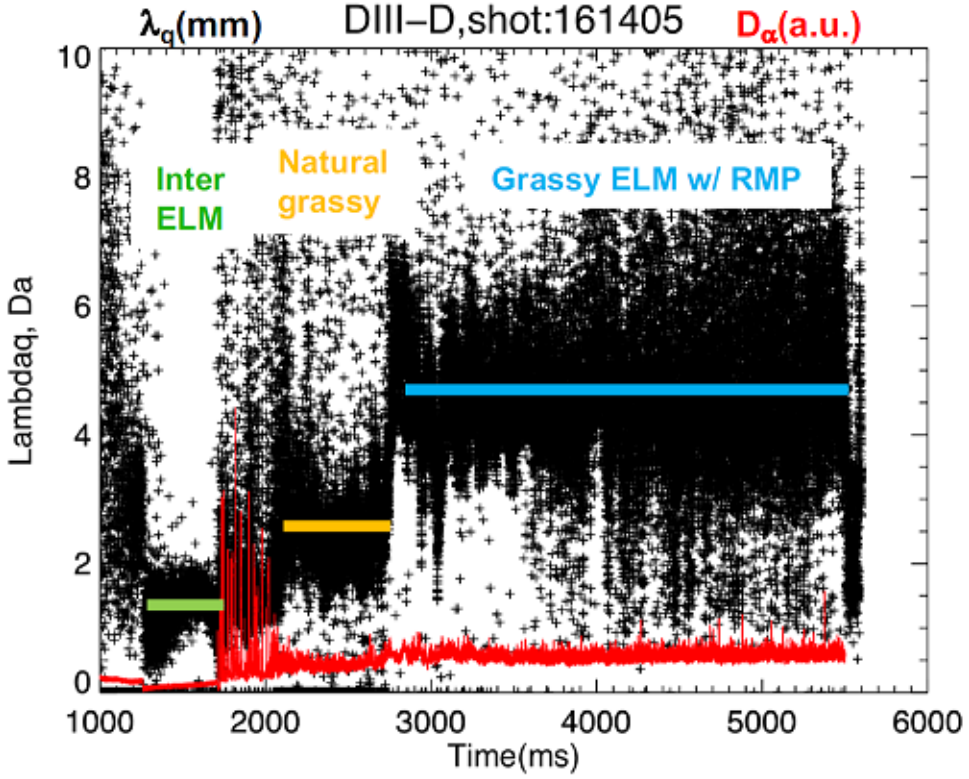

Figure 2. The Da signal (RED) and inner divertor heat flux width (Black) from the infrared IR camera measurement, which shows mixed ELM activities. From the ELM-free phase to the natural grassy ELM phase, the width increases about 2-3 times w/o RMP. The divertor heat flux width increases about 6 times w/RMP. The grassy ELM exhibit a reduced peak heat flux to the divertor, about ~20% higher than that during the ELM-free phase.

Figure 2:

Country or International Organization

United States

Affiliation

Lawrence Livermore National Laboratory

Authors: XU, Xueqiao (Lawrence Livermore National Laboratory); Mrs WANG, Xueyun (Peking University); Dr WANG, Huiqian (General Atomics, San Diego, CA 92186, USA); Mrs LI, Nami (Dalian University of Technology); Dr LI, Zeyu (General Atomics); Dr YAN, Ning (Institute of Plasma Physics, Chinese Academy of Science, Hefei, peoples Republic of China); XU, Guosheng (Institute of Plasma Physics, Chinese Academy of Sciences); Mrs HE, Xiaoxue (Dalian University of Technology); Mr DENG, Guozhong (Institute of Plasma Physics); Dr XIA, Tianyang (Institute of Plasma Physics); Dr ZHU, Ben (Lawrence Livermore National Laboratory); CHAN, Vincent S. (General Atomics); GUO, Houyang (General Atomics); Dr REN, Jun (University of Tennessee, Knoxville); Dr LASNIER, Charlie (Lawrence Livermore National Laboratory); NAZIKIAN, Raffi (Princeton Plasma Physics Laboratory); Dr ASHOURVAN, Arash (Princeton Plasma Physics Laboratory)

Presenter: XU, Xueqiao (Lawrence Livermore National Laboratory)

Session Classification: P7 Posters 7

Track Classification: Magnetic Fusion Experiments